Attenuation of a Shielded Rectangular Dielectric Rod Waveguide

Colin G. Wells, *Member, IEEE*, and James A. R. Ball, *Member, IEEE*

***Abstract*—The attenuation coefficient of a rectangular dielectric line enclosed by a rectangular shield is obtained by the use of a rigorous mode-matching method to calculate the required mode field intensity. The cross section of the waveguide is overlaid by a grid, and numerical integration is used to determine the power flow, dielectric, and conductor losses and respective attenuation coefficients. To obtain experimental verification, a length of waveguide was made into a resonator, and measured and calculated Q factors were compared. The results for the E_{11}^y mode show how the influence of the shield decreases with distance. This is relevant to the design of dielectric waveguide structures and in filter applications where dielectric resonators are used.**

***Index Terms*—Attenuation, dielectric waveguides, mode-matching methods, numerical analysis, shielding.**

I. Introduction

RECTANGULAR dielectric waveguides are used in integrated optics, millimeter-wave integrated circuits, and as transmission lines. Compared to metal waveguides, at millimeter-wave frequencies, they have lower propagation loss (depending on dielectric loss), lower cost and are easier to fabricate [4]. They are also significantly smaller [1]. Shielded square cross-sectional dielectric resonators are also used in filter applications, e.g., in multimode cubic dielectric-resonator filters [2].

The loss in rectangular dielectric waveguides is mostly due to that in the dielectric. However, if the waveguide is surrounded by a rectangular metallic shield (see Fig. 1), then the total loss of the waveguide will also include loss due to induced currents in the inner surface of the shield walls. In a recent paper [9], a modified version of the mode-matching method devised by Solbach and Wolf [7] (modified Solbach and Wolf (MSW) method) was used to find the propagation coefficients and field patterns of the hybrid modes of a shielded rectangular dielectric waveguide. In this paper, the calculated fields for the commonly used E_{11}^y mode will be employed to find the wall and dielectric losses of the waveguide and, hence, its attenuation. The effect of the proximity of the shield on the attenuation will also be evaluated.

II. Calculating the Attenuation Coefficient Using Mode Matching

The modes supported by a rectangular shielded dielectric rod waveguide were investigated using mode matching in a recent paper [9]. The cross section was divided into three separate regions, and the field within each region represented as a sum of basis functions particular to the region. Due to symmetry, it was only necessary to consider one quadrant of the cross section for which the mode-matching regions are as shown in Fig. 2. Continuity of the tangential fields was then enforced at the boundaries between the regions, allowing the amplitudes of the basis functions to be determined. Once this has been accomplished, the field components of any required mode can be calculated at any point in the cross section.

To calculate the power losses within the waveguide, the cross section is overlaid with a grid with lines spaced at $\triangle x$ and $\triangle y$, as illustrated in Fig. 2. Field values and power densities are calculated at each intersection of the grid lines, and the total power flow and power dissipation is found by numerical integration.

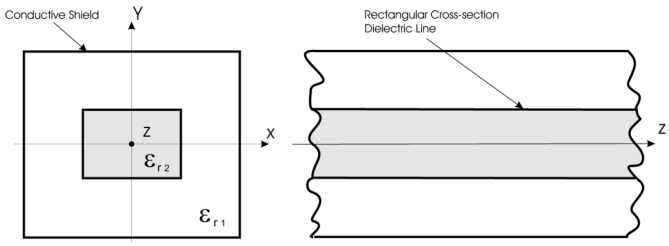

Fig. 1. Shielded dielectric rod waveguide.

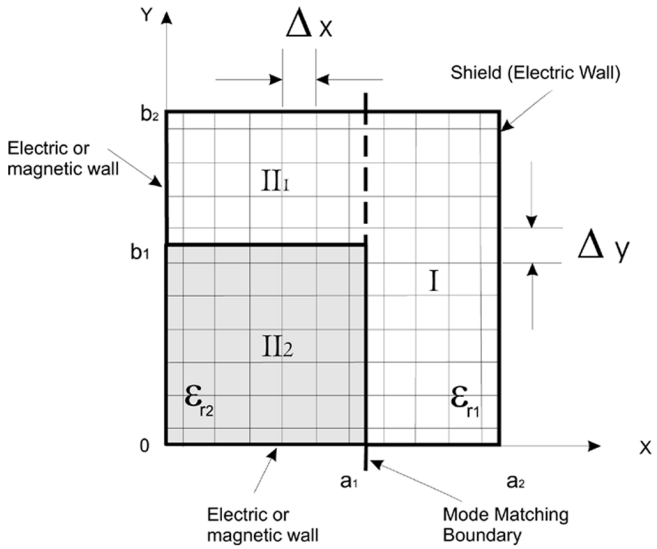

Fig. 2. One quadrant of the cross section showing the grid for power loss calculation.

Manuscript received June 7, 2005; revised January 23, 2006. The work of C. G. Wells was supported by the University of Southern Queensland under a scholarship.

The authors are with the Department of Engineering, University of Southern Queensland, Toowoomba, Qld., Australia.

Digital Object Identifier 10.1109/TMTT.2006.877056

From Poynting's theorem, the time average power P_0 over the full cross section $(z = 0)$ of a wave traveling in the z direction can be written as

$$P_0 = \frac{1}{2}\mathrm{Re}\left(4\int_0^{b_2}\int_0^{a_2} \mathbf{E}\times\mathbf{H}^*\cdot\hat{z}\,dx\,dy\right) \quad (1)$$

$$= \frac{1}{2}\mathrm{Re}\left(4\int_0^{b_2}\int_0^{a_2} \left(E_xH_y^* - E_yH_x^*\right)dx\,dy\right) \quad (2)$$

where "*" denotes a complex conjugate and the integration is over one quarter of the cross section.

Using numerical integration in the form of a Riemann sum, the total power flow is found by writing (2) as

$$P_0 \simeq 2\mathrm{Re}\left(\sum_{i=1}^{n}\left(E_{xI}^{(i)}H_{yI}^{*(i)} - E_{yI}^{(i)}H_{xI}^{*(i)}\right) + \sum_{j=1}^{m}\left(E_{xII1}^{(j)}H_{yII1}^{*(j)} - E_{yII1}^{(j)}H_{xII1}^{*(j)}\right) + \sum_{k=1}^{p}\left(E_{xII2}^{(k)}H_{yII2}^{*(k)} - E_{yII2}^{(k)}H_{yII2}^{*(k)}\right)\right)\cdot\Delta x\Delta y \quad (3)$$

where $i, j,$ and k identify the $n, m,$ and p nodes in regions $I, II_1,$ and II_2, respectively.

If the dissipation in the walls and dielectric is sufficiently small, the fields within the waveguide will be almost the same as in the lossless case. This allows both types of losses to be estimated from the lossless fields using the perturbation method [6].

The dielectric power loss per unit length over the cross section can be obtained from

$$P_d = \frac{\omega\varepsilon''\varepsilon_o}{2}4\int_0^{b_1}\int_0^{a_1}|\mathbf{E}(x,y,z)|^2dx\,dy \quad (4)$$

and

$$\varepsilon'' = \varepsilon'\tan\delta$$

where ε_o is the permittivity of free space, ε'' is the dielectric loss factor, ε' is the real part of the dielectric relative permittivity ε_{r2} in region II_2, and $\tan\delta$ is the dielectric loss tangent.

The numerical form of (4) is

$$P_d \simeq 2\omega\varepsilon''\varepsilon_o\cdot\sum_{k=1}^{p}\left(E_y^{(k)}E_y^{*(k)} + E_x^{(k)}E_x^{*(k)} + E_z^{(k)}E_z^{*(k)}\right)\cdot\Delta x\Delta y \quad (5)$$

where the index k identifies p nodes in region II_2.

The conductor loss per unit length in the shield walls can be obtained from

$$P_w = \frac{1}{2}R_S\int_C|\mathbf{H}_{\tan}|^2dl \quad (6)$$

and

$$R_S = \sqrt{\frac{\omega\mu_o}{2\sigma}}$$

where $\bar{H}_{\tan}$ is the magnetic field tangential to the walls, R_S is the wall surface resistance, μ_o is the permeability of free space, and σ is the conductivity of the wall material. Integration contour C corresponds to the inner perimeter of the guide wall in the waveguide cross section. The numerical form becomes

$$P_w \simeq 2R_S\left(\sum_{t=1}^{T}\left(H_x^{(t)}H_x^{*(t)} + H_z^{(t)}H_z^{*(t)}\right)\Delta x + \sum_{s=1}^{S}\left(H_y^{(s)}H_y^{*(s)} + H_z^{(s)}H_z^{*(s)}\right)\Delta y\right) \quad (7)$$

where t identifies T nodes, on the top shield boundary $(0 \le x \le a_2, y = b_2)$ spaced Δx apart, and the index s identifies S points on the right-hand-side shield boundary $(0 \le y \le b_2, x = a_2)$ with spacing Δy. Also in (3), (5), and (7), each component of $\mathbf{E}$ or $\mathbf{H}$, at a point, is the sum of a number of basis function values calculated using the MSW method.

By substituting the spatial grid component values into these equations, a close approximation to the power flow and losses can be obtained for the structure. Since (3), (5), and (7) are obtained from 4× the quarter structure of Fig. 2, duplication of common points at the boundaries must be taken into account.

From [6], the attenuation coefficient due to dielectric loss and shield wall loss can then be calculated using

$$\alpha = \frac{P_l}{2P_0} = \frac{P_d + P_w}{2P_0} = \alpha_d + \alpha_w \quad (8)$$

where $P_d, \alpha_d,$ and P_w, α_w are the dielectric loss and attenuation and shield wall loss and attenuation, respectively.

In practice, conductor loss is increased by surface roughness, and this is normally taken into account by multiplying the theoretical value of the surface resistance by a roughness factor [5].

III. Alternative Method of Calculating the Attenuation Coefficient Due to Dielectric Loss

Another way of calculating the attenuation due to dielectric loss (α_d) only is to calculate it directly using the MSW method. In this procedure, the lossless propagation coefficient (β_z) is calculated first. The loss factor ε'' is then determined from the loss tangent, and included to give a complex permittivity of the dielectric. The program can then be run again using a range of complex propagation coefficients γ_z. These consist of the lossless β_z and a range of α_z values. A value of α_d is then determined by finding that value of α_z for which the determinant of the mode-matching equation matrix is closest to zero. This would normally be the start of an iterative process in which α_z and β_z are varied alternatively until the propagation coefficient converges to a value of sufficient accuracy. It was found, however, that during this iterative procedure, the variation in β_z was insignificant and, thus, only the initial lossless β_z value was required.

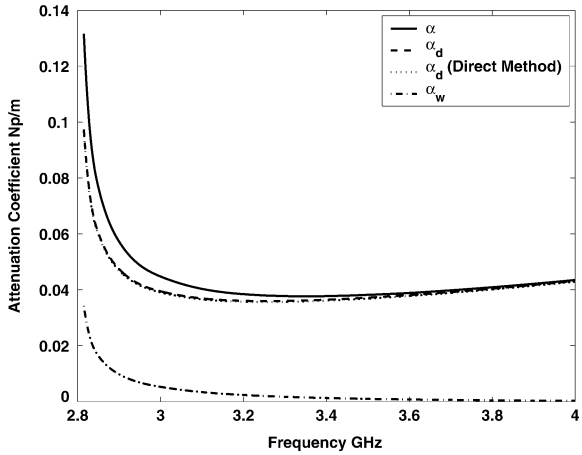

Fig. 3. Attenuation coefficient versus frequency for the E_{11}^y mode. The SDR is $\mathrm{SDR} = a_2/a_1 = 2$.

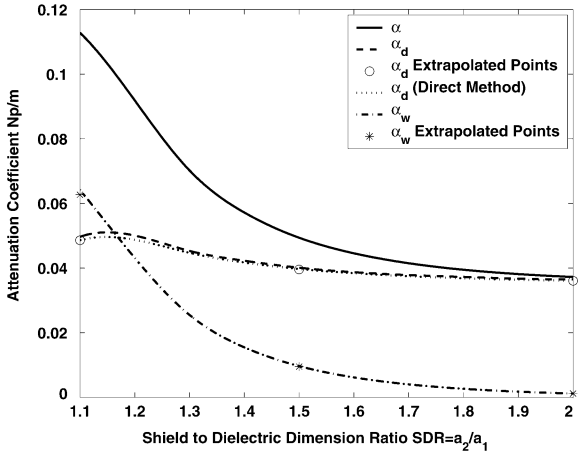

Fig. 4. Attenuation coefficient versus SDR for the E_{11}^y mode. The frequency is 3.4 GHz.

The perturbation method using the grid is preferred to the above direct method, as it can be used to find both shield wall loss and dielectric loss. It is also much faster to compute. However, since fields from the lossless solution are used to estimate the dissipation, some additional error is involved. In Section IV, dielectric loss results obtained by both methods are compared to show that the additional error cost of the perturbation approximation is negligible.

IV. Discussion of Calculated Results

The attenuation coefficients created by the dissipation within the dielectric and shield walls were calculated for the commonly used E_{11}^y mode using the grid method described in Section II. The dielectric rod material is barium tetratitanate for which the loss tangent is specified by the manufacturer (picoFarad, Anaheim, CA) as

$$\tan\delta = \text{Frequency(GHz)}/3 \times 10^4. \tag{9}$$

This material was also used to obtain the experimental results presented later. A surface roughness factor of unity has been assumed for the metal shield. The attenuation coefficient verses frequency (beginning near cutoff) with a shield to dielectric dimension ratio (SDR), $\mathrm{SDR} = a_2/a_1 = 2$, is shown in Fig. 3. The plot of the attenuation coefficient verses SDR with the frequency at 3.4 GHz is shown in Fig. 4.

For the E_{11}^y mode shown in Fig. 4, as shield size increases relative to the dielectric, α_w is gradually dominated by a relatively constant α_d. This indicates that when using a dielectric with a relative permittivity of around 37, choosing an $\mathrm{SDR} > 2$ will minimize the shield conductor loss.

The size of grid used in these plots was 51×51 points for one-quarter of the structure. The values marked with "$\circ$" and "*" on the plots are generated from an extrapolation of the convergence of the attenuation coefficient with an increase in grid size. The maximum grid used in this convergence process was 501×501. The comparison of these values show that a grid size of 51×51 (very efficient to compute) should be of sufficient accuracy for SDR values down to 1.1. Below this, larger grid sizes will be required.

To estimate the extra error due to the perturbation approximation, which is inherent in the grid method, α_d of the E_{11}^y mode was also calculated directly using the MSW method, as described in Section III. The results are shown in Figs. 3 and 4, and show excellent agreement with the grid method extrapolated values.

As $\mathrm{SDR} \Rightarrow 1$, the E_{11}^y mode becomes TE_{10}, and the E_{21}^x/E_{12}^y coupled modes become the TM_{11} mode. The TE_{10}- and TM_{11}-like qualities of these modes, in a cross section of the dielectric region, can be seen in Figs. 5 and 6, respectively. Hence, a further check of the grid method was performed by analytically calculating the perturbation approximations for α_w and α_d in a square cross-sectional waveguide completely filled with dielectric [6]. These were compared to those obtained from the grid method as the SDR value is brought very close to 1. To obtain the best accuracy, the grid method values, as mentioned before, were obtained from an extrapolation of the convergence of the attenuation coefficient with an increase in grid size. The dimensions of the waveguide used were the same as the dielectric rod used in experimental measurement, i.e., a 12.05-mm square cross section ($\varepsilon_r = 37.13$) at a frequency of 3.4 GHz and with $\tan\delta$ calculated for the dielectric at that frequency. The results, shown in Table I, show a difference of less than 2%.

V. Measurement Technique

To verify the grid mode-matching method for finding loss, comparisons of calculated and measured unloaded Q were made for the E_{11}^y mode using two sizes of resonator.

The resonators consisted of a square cross-sectional barium tetratitanate dielectric rod (12.05×12.05 mm) placed in a square cross-sectional brass waveguide of the same length L (153.3 mm). Brass end plates were added to the waveguide, also in contact with ends of the rod, to form the resonators. Measurements of the reflection coefficient were made using a vector network analyzer that was lightly coupled to the resonators by a probe mounted at the midpoint, as in Fig. 7. To

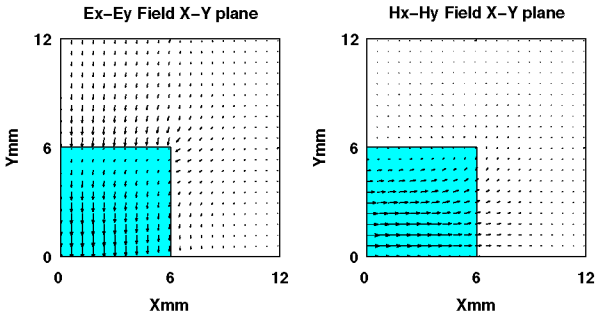

Fig. 5. Electric and magnetic field patterns in the xy-plane for the E_{11}^{y} mode. (Color version available online at http://ieeexplore.ieee.org.)

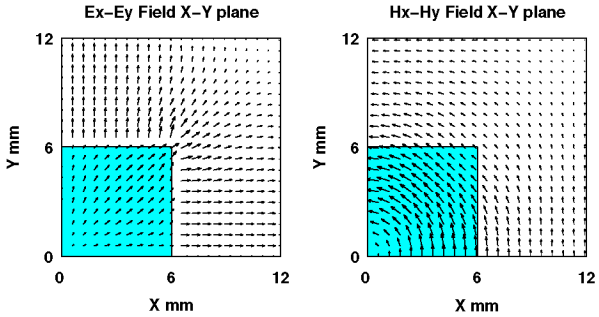

Fig. 6. Electric and magnetic field patterns in the xy-plane for the coupled E_{21}^{x}/E_{12}^{y} modes. For clarity, the electric field intensity in the dielectric is $x5$. (Color version available online at http://ieeexplore.ieee.org.)

TABLE I
COMPARISON OF EXTRAPOLATED GRID METHOD ATTENUATION COEFFICIENT RESULTS (Np/m) FOR THE SHIELDED RECTANGULAR DIELECTRIC WAVEGUIDE, AT SDR $=$ 1, AND THOSE CALCULATED FOR DIELECTRIC FILLED RECTANGULAR WAVEGUIDE ($a_1 = b_2 = 6.025$ mm, $\varepsilon_{r2} = 37.13$, Frequency $= 3.4$ GHz)

	TE_{10}	E_{11}^{y} Grid Method	%
α_w	0.08447	0.0837	-0.9
α_d	0.03077	0.0306	-0.6
	TM_{11}	E_{21}^{x}/E_{12}^{y} Grid Method	%
α_w	0.1486	0.147	-1.1
α_d	0.04659	0.0458	-1.7

provide consistent results, the same dielectric rod was actually used in both resonators. The waveguides cross sections were 23.8×23.8 mm and 18×18 mm, giving SDR values of 1.98 and 1.49, respectively.

The measurements of the unloaded Q were carried out using a form of the amplitude reflection method [3].

The unloaded Q of a resonator can be calculated from

$$Q = \frac{\omega_0 W}{P_{Cd} + P_{Cw} + P_e} \tag{10}$$

where ω_0 is the frequency at resonance, W is $4\times$ the energy stored in the three regions of Fig. 2 over the resonator length, and

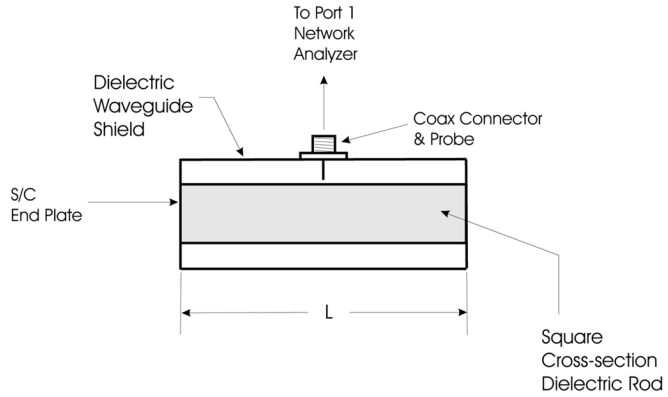

Fig. 7. Dielectric resonator used for the measurement of unloaded Q.

P_{Cd}, P_{Cw}, and P_e are the dielectric, wall and end plate losses in the resonator, respectively.

The total energy stored in the resonator over the full cross section can be calculated from

$$W = \frac{\varepsilon_0}{2} 4 \int_0^L \int_0^{b_2} \int_0^{a_2} \varepsilon'(\mathbf{E} \cdot \mathbf{E}^*) dx\, dy\, dz \tag{11}$$

and the propagation coefficient will be

$$\beta_z(N) = \frac{N\pi}{L} \tag{12}$$

where N is the number of half-wavelengths of the resonant mode under investigation. Furthermore, the z variation of the components of $\mathbf{E}$ in this type of resonator will be of the form $2\sin\beta_z z$ or $2\cos\beta_z z$. After integration with respect to z, (11) can be written as

$$W = L\varepsilon_0 4 \int_0^{b_2} \int_0^{a_2} \varepsilon'(\mathbf{e} \cdot \mathbf{e}^*) dx\, dy \tag{13}$$

where $\mathbf{e}$ is a function of the transverse coordinates only. In Reimann sum form,

$$\begin{aligned} W \simeq\ & 4L\varepsilon_0 \\ & \cdot \left(\sum_{i=1}^{n} \left(e_{xI}^{(i)} e_{xI}^{*(i)} + e_{yI}^{(i)} e_{yI}^{*(i)} + e_{zI}^{(i)} e_{zI}^{*(i)} \right) \right. \\ & + \sum_{j=1}^{m} \left(e_{xII1}^{(j)} e_{xII1}^{*(j)} + e_{yII1}^{(j)} e_{yII1}^{*(j)} + e_{zII1}^{(j)} e_{zII1}^{*(j)} \right) \\ & \left. + \varepsilon' \sum_{k=1}^{p} \left(e_{xII2}^{(k)} e_{xII2}^{*(k)} + e_{yII2}^{(k)} e_{yII2}^{*(k)} + e_{zII2}^{(k)} e_{zII2}^{*(k)} \right) \right) \\ & \cdot \Delta x \Delta y \end{aligned} \tag{14}$$

where i, jm, and k identify the n, m, and p nodes in regions I, II_1, II_2, respectively.

TABLE II
COMPARISON OF CALCULATED AND MEASURED Q VALUES FOR THE 153.3 -mm-LONG SQUARE CROSS-SECTIONAL DIELECTRIC ROD RESONATOR AT N HALF-WAVELENGTHS ($a_1 = b_1 = 6.025$ mm, $a_2 = b_2 = 11.9$ mm AND 9 mm)

SDR (a_2/a_1)	N	Measured Frequency (GHz)	Measured Unloaded Q	Calculated Unloaded Q	% Q Diff.
1.49	7	2.9731	3368	3373	-0.15
	8	2.9973	3704	3589	+3.2
	17	3.7589	4816	4924	-2.2
	20	4.1135	4315	4927	-12.4
1.98	7	2.8371	5001	5097	-1.9
	13	3.2907	4851	5743	-15.5
	17	3.7313	5179	5507	-6.0
	18	3.8508	5054	5412	-6.6

Alternatively, the energy stored in the cavity may be obtained from the power flow in the infinite waveguide (3)

$$W = \frac{2LP_0}{v_g} \tag{15}$$

where v_g is the group velocity, obtainable numerically.

Similarly, the dielectric and wall losses within the cavity can be obtained from the corresponding waveguide losses per unit length as follows:

$$P_{Cd} = 2LP_d \tag{16}$$

$$P_{Cw} = 2LP_w. \tag{17}$$

The end-plate loss, for both ends and the full cross section of the resonator, can be calculated from

$$P_e = 16R_s \int_0^{b_2}\int_0^{a_2} |\mathbf{h}_t|^2 dx\, dy \tag{18}$$

which becomes in Reimann sum form

$$P_e \simeq 16R_s \sum_{i=1}^{n} \left(h_x^{(i)} h_x^{*(i)} + h_y^{(i)} h_y^{*(i)}\right) \Delta x \Delta y. \tag{19}$$

VI. COMPARISON OF CALCULATED AND MEASURED RESULTS

The reflection coefficient values for resonances of the E_{11}^y mode were measured over a frequency range from cutoff to 4.2 GHz. When comparing the measured Q factor results to calculated values, it is necessary to account for surface roughness. The average surface roughness due to the milling process was estimated as 3.2 μm. Given that the shield material is brass containing 38% zinc with a conductivity of 1.57×10^7 Ωm, a surface roughness factor of approximately 1.7 is predicted from [5]. The method used in [5] assumes that the surface profile shows a regular variation, e.g., a sawtooth. The actual surface profile is likely to be more complicated than this. Therefore, a surface roughness factor of 2 was used to calculate the Q-factor values. A comparison of measured and calculated values is shown in Table II. Percentage differences of the measured values with respect to the calculated values are shown in the right-hand-side column. From this, it can be seen that, on average, the measured Q-factor values are too low by approximately 5%. The most probable reason for this is the flange contact resistance of the short-circuit end plates, which were bolted on, not soldered [8].

Not all possible resonances were able to be measured. It was found that some resonances did not couple well to the probe and, thus, were too noisy. Other resonances were found to be affected by significant coupling to the degenerate mode E_{11}^x, which made accurate unloaded Q calculations impossible at these frequencies.

Mode charts for the first few modes to propagate are shown in Figs. 8 and 9 for SDRs of 1.49 and 1.98, respectively. The "○" points show the propagation coefficients from (12) plotted

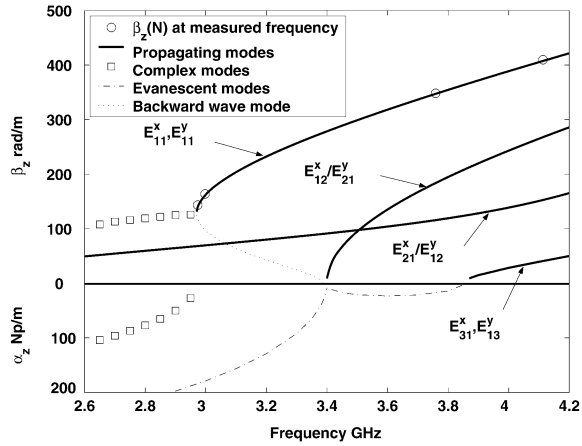

Fig. 8. Calculated propagation coefficient values for the first few modes to propagate, with measurements of the E_{11}^y mode superimposed. Shield dimension ratio $\mathrm{SDR} = 1.49$.

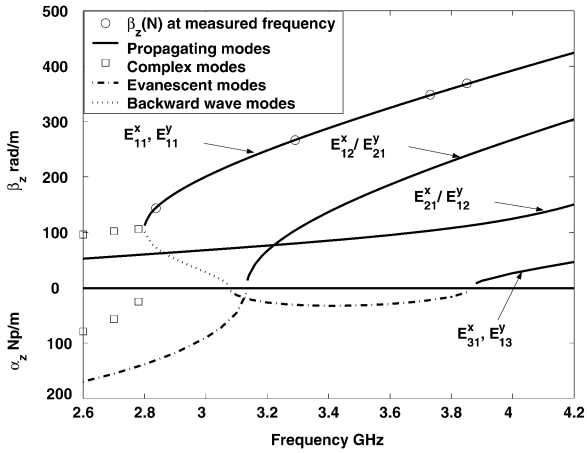

Fig. 9. Calculated propagation coefficient values for the first few modes to propagate, with measurements of the E_{11}^y mode superimposed. Shield dimension ratio $\mathrm{SDR} = 1.98$..

against the measured frequencies of the resonances so that comparison with calculation can be made. The differences between measured and calculated frequencies at the same N propagation values are less than 1% for both resonators.

VII. Conclusion

A numerical method for finding the attenuation coefficient of a shielded rectangular dielectric rod waveguide has been presented. The technique is based on the perturbation method in conjunction with field calculations using the MSW mode-matching method described in [9]. The effect of frequency and the proximity of the shield to the dielectric rod, on the attenuation coefficient, has been shown for the E_{11}^{y} mode. It is believed that these results for the rectangular dielectric rod waveguide have not previously appeared in the literature. The method is confirmed by a close comparison with a direct method for calculating the attenuation coefficient due to the dielectric and also with analytically calculated values for a rectangular waveguide completely filled with dielectric. The method is also validated by good comparison of the measured and calculated Q values of the shielded dielectric rod waveguide when used as a resonator.

The results of this paper will be relevant to the design of dielectric waveguide structures and in filter applications where dielectric resonators are used.

Acknowledgment

The prototype dielectric shielded line was manufactured at the University of Southern Queensland (USQ) Mechanical Engineering Workshop by C. Galligan.

References

[1] A. G. Engel, Jr. and L. P. B. Kathi, "Low loss monolithic transmission lines for submillimeter and terahertz frequency applications," *IEEE Trans. Microw. Theory Tech.*, vol. 39, no. 11, pp. 1847–1854, Nov. 1991.

[2] I. Hunter, *Theory and Design of Microwave Filters*, ser. Electromagnetic Wave Series. London, U.K.: IEE Press, 2001.

[3] D. Kajfez and E. J. Hwan, "Q-factor measurement with network analyzer," *IEEE Trans. Microw. Theory Tech.*, vol. MTT-32, no. 7, pp. 666–670, Jul. 1984.

[4] D. Lioubtchenko, S. Tretyakov, and S. Dudorov, *Millimeter-Wave Waveguides*. Boston: Kluwer, 2003.

[5] S. P. Morgan, "Effect of surface roughness on eddy current losses at microwave frequencies," *J. Appl. Phys.*, vol. 20, no. 4, pp. 352–362, 1949.

[6] D. M. Pozar, *Microwave Engineering*, 2nd ed. New York: Wiley, 1998.

[7] K. Solbach and I. Wolf, "The electromagnetic fields and the phase constants of dielectric image lines," *IEEE Trans. Microw. Theory Tech.*, vol. MTT-26, no. 4, pp. 266–274, Apr. 1978.

[8] P. I. Somlo, "The effect of flange loss on the reflection coefficient of reduced height," *IEEE Trans. Microw. Theory Tech.*, vol. MTT-27, no. 9, pp. 795–797, Sep. 1979.

[9] C. G. Wells and J. A. R. Ball, "Mode matching analysis of a shielded rectangular dielectric rod waveguide," *IEEE Trans. Microw. Theory Tech.*, vol. 53, no. 10, pp. 3169–3177, Oct. 2005.

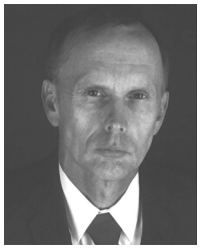

Colin G. Wells (S'02–M'05) was born in Sydney, Australia, on April 3, 1951. He received the B.Eng. degree in electrical and electronic engineering and Ph.D. degree from the University of Southern Queensland, Toowoomba, Qld., Australia, in 2002 and 2006, respectively. His doctoral dissertation concerned the design of microwave components and filters using the mode-matching technique.

James A. R. Ball (M'81) was born in Guildford, U.K., on February 11, 1943. He received the B.Sc. degree in engineering from Leicester University, Leicester, U.K., in 1964, the M.Sc. degree in physics from the University of London, London, U.K., in 1968, and the Ph.D. degree in electrical engineering from the University of Queensland, Queensland, Qld., Australia, in 1988.

From 1964 to 1969, he was a Microwave Engineer with EMI Electronics U.K., where he was involved with stripline and waveguide component design. From 1969 to 1971, he was with Amalgamated Wireless (Australasia), where he was involved with the design of low-frequency and UHF filters, and the testing of delta modulation and UHF radio links. In 1971, he joined the University of Southern Queensland, Toowoomba, Qld., Australia, where he is currently an Associate Professor of electrical, electronic and computer engineering with the Department of Engineering. His research interests are in the areas of microwave components, devices and measurements, and the numerical solution of electromagnetic field problems.